ADVANCED ENGINEERING MATERIALS
www.aem-journal.com

Utilizing the Sensitization Effect for Direct Laser Writing in a Novel Photoresist Based on the Chitin Monomer N-acetyl-D-glucosamine

Dominic T. Meiers, Maximilian Rothammer, Maximilian Maier, Cordt Zollfrank,* and Georg von Freymann**

The great flexibility of direct laser writing (DLW) arises from the possibility to fabricate precise three-dimensional structures on very small scales as well as the broad range of applicable materials. However, there is still a vast number of promising materials, which are currently inaccessible requiring the continuous development of novel photoresists. Herein, a new bio-sourced resist is reported that uses the monomeric unit of chitin, N-acetyl-D-glucosamine, paving the way from existing hydrogel resists based on animal carbohydrates to a new class of non-hydrogel ones. In addition, it is shown that the combined use of two photoinitiators is advantageous over the use of a single one. In this approach, the first photoinitiator is a good two-photon absorber at the applied wavelength, while the second photoinitiator exhibits poor two-photon absorbtion abilities, but is better suited for cross-linking of the monomer. The first photoinitiator absorbs the light acting as a sensitizer and transfers the energy to the second initiator, which subsequently forms a radical and initializes the polymerization. This sensitization effect enables a new route to utilize reactive photointiators with a small two-photon absorption cross section for DLW without changing their chemical structure.

1. Introduction

Since its invention in the mid 1990s[1] and its commercialization a decade afterward, direct laser writing (DLW) rapidly became the most versatile tool for fabricating three-dimensional structures from submicron to centimeter scales. Today, direct laser written structures find application in almost all fields requiring structures with microscopic features such as microoptics,[2–4] microfluidics,[5–7] biomimetics,[8–10] and life science.[11–13]

In contrast to other optical lithography techniques, DLW relies on the simultaneous absorption of two photons, i.e., a nonlinear process, to initialize the polymerization of an appropriate photoresist. In consequence, the absorption exceeds the polymerization threshold only in the tight focus of a femtosecond laser beam. This limits the polymerized area in all three dimensions and therefore enables the fabrication of almost arbitrary three-dimensional structures with feasible feature size and resolution (i.e., smallest distance between two features) below 100 and 500 nm, respectively, depending on the setup.[14]

In addition to optimizing the underlying technology to improve resolution and fabrication speed, the range of available materials that can be patterned by DLW has rapidly expanded over the last decade to meet different applications. Originally starting with a few polymer-based resists, today there is a whole range of such resists designed for different length scales, writing speeds, optical, mechanical, or surface properties.[15–19] However, DLW-suitable photoresists are not limited to traditional polymer-based ones, but it is also possible to structure ceramics,[20,21] metals,[22,23] hydrogels,[24,25] glass,[26] and biomaterials.[27–32]

In general, biomaterials can be divided into three classes, namely lipids, carbohydrates, and proteins as well as on their origin, i.e., animal or plant sourced. In the field of animal-based materials for DLW, the vast majority relies on proteins such as bovine serum albumin, silk fibroin, and different types of collagen to name just a few (see reference[30] for a more comprehensive overview). Beside proteins, carbohydrates such as hyaluronan[31,33,34] and chitosan[32] are successfully

D. T. Meiers, G. von Freymann
Physics Department and Research Center OPTIMAS
RPTU Kaiserslautern-Landau
67663 Kaiserslautern, Germany
E-mail: dmeiers@rptu.de; georg.freymann@physik.uni-kl.de, georg.von.freymann@itwm.fraunhofer.de

M. Rothammer, M. Maier, C. Zollfrank
Chair for Biogenic Polymers
Technische Universität München
94315 Straubing, Germany
E-mail: cordt.zollfrank@tum.de

G. von Freymann
Department of Materials Characterization and Testing
Fraunhofer Institute for Industrial Mathematics ITWM
67663 Kaiserslautern, Germany

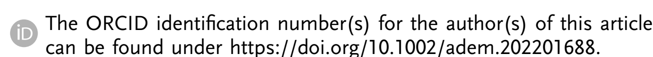
The ORCID identification number(s) for the author(s) of this article can be found under https://doi.org/10.1002/adem.202201688.

© 2023 The Authors. Advanced Engineering Materials published by Wiley-VCH GmbH. This is an open access article under the terms of the Creative Commons Attribution License, which permits use, distribution and reproduction in any medium, provided the original work is properly cited.

DOI: 10.1002/adem.202201688

15272648, 2023, 11, Downloaded from https://onlinelibrary.wiley.com/doi/10.1002/adem.202201688 by Rheinland-Pfälzische Technische Universität Kaiserslautern-Landau, Wiley Online Library on [22/04/2024]. See the Terms and Conditions (https://onlinelibrary.wiley.com/terms-and-conditions) on Wiley Online Library for rules of use; OA articles are governed by the applicable Creative Commons License

applied as direct laser writable hydrogels. Up to date research is largely focused on soft materials such as hydrogels since they can imitate the extracellular matrix enabling numerous biomedical applications, e.g., tissue engineering or drug delivery.[35,36]

However, alongside soft tissues nature offers a great variety of rigid materials, where, e.g., the polysaccharides cellulose and chitin serve as the main building block of wood cells and arthropods' hard shell, respectively.[37] In addition to its mechanical properties, chitin is also widely used by nature as a dielectric material in nanostructures exhibiting structural coloration.[38] While plant-based carbohydrates such as cellulose can be already patterned by DLW,[27,39] the available animal-based carbohydrates are currently limited to hydrogels.[31–34]

Here, we present the synthesis of a novel, functionalized derivative of the monomeric unit of chitin N-acetyl-D-glucosamine (NAG) which can be applied in a DLW-suitable photoresist. Thereby, the reported resist expands the existing hydrogel resists by a nonhydrogel formulation paving the way to a new class of bio-based photoresist with animal origin. Moreover, this photoresist is based on the monosaccharide NAG and therefore uses a low molecular compound compared to other common bio-based resists.[27,31,32,40]

The NAG is functionalized through the addition of methacrylic side groups, which can be cross-linked by an appropriate photoinitiator. While it is possible to structure the resist with a single photoinitiator, we demonstrate that the mixture of two different types is advantageous. Thereby, a similar principle is used as applied in pigmented UV curing, where the pigments in a lacquer show a stronger UV absorption than the photoinitiator. This shielding effect can be overcome by adding a sensitizer absorbing at a different (longer) wavelength, which is capable to transfer the absorbed energy to the photoinitiator forming highly reactive radicals.[41] The curing speed for pigmented lacquers can be largely increased using this sensitization effect.[42]

In case of photoresists, there is no shielding issue, but a mismatch between the used wavelength and the two-photon absorption (TPA) maximum of the photoinitiator leading to a small TPA cross section (TPCS). Therefore, we mix a sensitizer possessing a TPA maximum close to the used wavelength with a photoinitiator having a maximum noticeably below the applied wavelength, but being more effective to cross-link the monomer. As reported here, such a mixture indeed outperforms resists containing either solely a sensitizer or a photoinitiator.

2. Results and Discussion

2.1. Chemical Modification of N-acetyl-D-glucosamine

To provide photo-cross-linking capabilities to the monosaccharide NAG, unsaturated side groups are introduced via *N,N*-dicyclohexylcarbodiimide-coupled esterification during the synthesis. Methacrylic acid anhydride was employed for a functionalization of the hydroxyl groups of NAG and resulted into methacrylated N-acetyl-D-glucosamine (MANAG). However, exact positions of functionalization cannot be unambiguously determined due to overlapping signals, complex patterns, and a poor resolution achieved in the nuclear magnetic resonance (NMR) spectra (see Supporting Information). The reactive methacrylic moiety is essential for a subsequent photopolymerization reaction.

Fourier transform infrared spectroscopy (FTIR) analyses of NAG and MANAG verify the successful esterification of NAG with the unsaturated anhydride. The most characteristic intensities of absorption bands of NAG are displayed in **Figure 1**.

The absorption bands at 1624 and 1546 cm^{-1} correspond to the amide I and amide II modes of the amide carbonyl group in secondary amides, respectively.[43–48] The amide I band is mainly caused by C═O stretching vibrations and by a minor ratio of N─H bending and C─H and C─N stretching vibrations of amides.[49,50] The amide II band is assigned to N─H bending and some C─N stretching vibrations.[49–51] The bands at 3453 and 3322 cm^{-1} represent the O─H and N─H stretching vibrations.[45,47,52] C─O─C antisymmetric bridge oxygen stretching vibrations, C─O bond stretching vibrations, antisymmetric in-phase ring vibrations, and C─O─H stretching vibrations are located at 1125, 1049, and 1018 cm^{-1}.[45–47,51,52] New bands arise at 1721 and 812 cm^{-1} after the methacrylation reaction. The band at 1721 cm^{-1} correlates to the carbonyl C═O stretching vibrations of the ester[43,46,49,53] and therefore verifies a successful functionalization of NAG. The C═CH_2 out of plane deformation vibration of the methacrylate group appears at 812 cm^{-1}[27,53] and confirms the presence of carbon double bonds. Furthermore, a decrease of the absorption band at 3453 cm^{-1} corresponding to the hydroxyl groups is observable comparing the NAG and MANAG spectra. This confirms substitution at the OH groups by methacrylate groups.

Photo-cross-linking of MANAG results in a high decrease of the methacrylic carbon double bond ν(C═C) intensity at 812 cm^{-1}, indicating a consumption of the double bonds during polymerization of the monomers.

Moreover, the evaluation of the ^{1}H and ^{13}C NMR spectra also validates an effective methacrylation of NAG. The characteristic ^{13}C NMR signals of MANAG and NAG are depicted in **Table 1**. NAG is identified by the signals at 170.0, 91.1–54.8, and

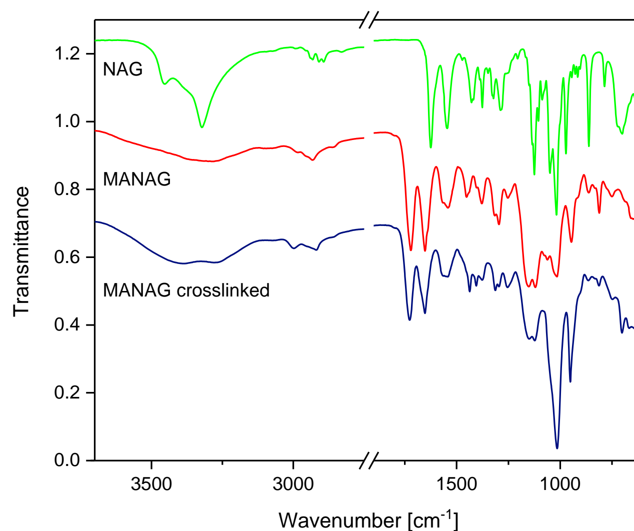

Figure 1. FTIR spectra of NAG, MANAG, and crosslinked MANAG. The spectra are vertically shifted for better readability.

 © 2023 The Authors. Advanced Engineering Materials published by Wiley-VCH GmbH

Table 1. Signal assignment for the ^{13}C NMR spectra of NAG and MANAG, analyzed in DMSO-d.

Sample	Assignment δ [ppm]						
	C=O (NAG)	C=O (MANAG)	C=C	C=C	C1—C6	CH_3 (NAG)	CH_3 (MANAG)
NAG	170.0	–	–	–	91.1–54.8	23.2	–
MANAG	169.8	166.9	136.3	126.3	91.6–54.8	23.2	18.6

23.2 ppm. The signals from 91.1 to 54.8 ppm are assigned to the C1—C6 atoms of the glucose backbone of the monosaccharide.[54] 170.0 ppm represents the ester and 23.2 ppm the methyl group of the N-acetate moiety, respectively.[54] After the synthesis, new peaks arise around 166.9 ppm, which reveal the esterification of NAG with methacrylic acid anhydride at several positions.[27,54] The signals corresponding to the carbon double bond are located around 136.3 and 126.3 ppm.[27] Furthermore, the peaks for the CH_3 group of the methacrylic side group are detected around 18.6 ppm.[53] The splitting of the corresponding signals indicates an esterification at various positions of the NAG backbone.

Additionally, ^{1}H NMR spectra affirm a successful methacrylation by the appearance of further signals compared to NAG. The signals at 5.98 and 5.65 ppm refer to the vinyl protons of the carbon double bond,[46,53] while the peak at 1.85 ppm is assigned to the methyl protons of the methacrylic moiety, respectively.[53,55]

Due to some persistent impurities of the applied coupling reagents within the MANAG product, a detailed determination of the degree of methacrylation was impossible, but elemental analysis measurements of the synthesized MANAG indicate a value in the range of about 1.5–3.0. Therefore, the resulting polymer networks after polymerization are probably a mixture of linear polymers in case of MANAG monomers with a degree of methacrylation of 1.0 and a cross-linked polymer network, which consists of MANAG molecules with a degree of methacrylation above 1.0. This may result in areas revealing different cross-linking densities and hence creating a rough surface of the written architectures.

MANAG is cross-linkable via TPA using a DLW-setup as well via one-photon absorption employing a UV lamp ($\lambda = 254$ and 365 nm).

The synthesized MANAG is soluble in dimethyl sulfoxide (DMSO), dimethylformamide, and dimethylacetamide, whereas the cross-linked monosacharides are insoluble in common organic solvents.

2.2. Direct Laser Writing of NAG-Based Structures

The functionalized NAG is dissolved in DMSO and mixed with different photoinitiators to obtain feasible NAG-based

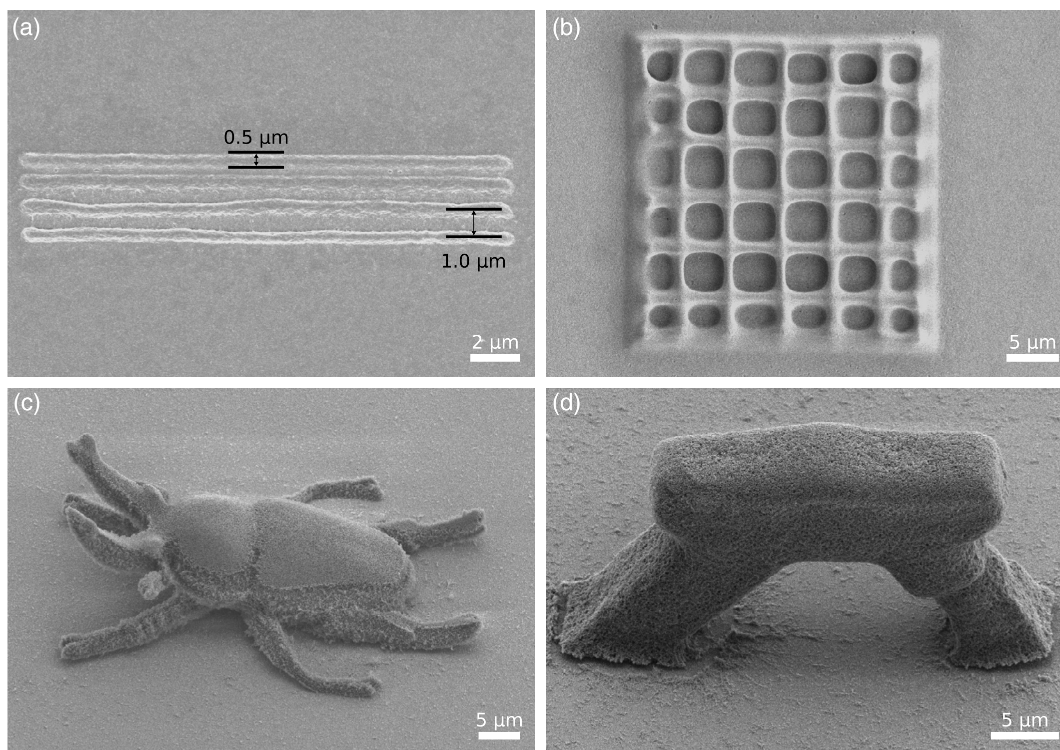

Figure 2. SEM micrographs: a) printed lines revealing a micron resolution and a submicron feature size. The lines are written at a speed of 10 µm s^{-1} with 30% laser power in a resist containing Irgacure 369. b) Fabricated 2D grid structure at a writing speed of 50 µm s^{-1} and 90% laser power using Irgacure 819 as photoinitiator. c) A 3D model of a rainbow stag beetle written at 1000 µm s^{-1} and 90% laser power in a photoresist containing Irgacure 369. d) Printed arch at 100 µm s^{-1} and 30% laser power using Irgacure 819, revealing a free standing structure. The images in (a), (b) show top views on the respective structure while the images in (c), (d) depict side views at 45°.

© 2023 The Authors. Advanced Engineering Materials published by Wiley-VCH GmbH

15272648, 2023, 11, Downloaded from https://onlinelibrary.wiley.com/doi/10.1002/adem.202201688 by Rheinland-Pfälzische Technische Universität Kaiserslautern-Landau, Wiley Online Library on [22/04/2024]. See the Terms and Conditions (https://onlinelibrary.wiley.com/terms-and-conditions) on Wiley Online Library for rules of use; OA articles are governed by the applicable Creative Commons License

photoresists. In preliminary tests, the commercial photoinitiators Irgacure 369 and Irgacure 819 provide the best structure quality and hence are used for investigating the capability of the NAG-based photoresists. In contrast, potent photoinitiators for DLW at 780 nm such as DETC (see Supporting Information) turn out to be not suitable for structuring NAG-based resists.

Figure 2 shows a selection of different structures, which can be fabricated with NAG-based resists using Irgacure 369 (a,c) or Irgacure 819 (b,d) as photoinitiator. Fabrication of typical 2D structures such as lines and grids is depicted in Figure 2a,b. The lines in Figure 2a reveal a lateral resolution of about 1 μm and a feature size of around 500 nm, which is comparable to the specifications of a previously reported cellulose-based photoresist.[27] Achieving feature sizes and a resolution on the scale of about one micron is important for the fabrication of biomimetic structures as shown by the wide range of functional nano- and microstructures found for example in insects.[38]

While 2D structures can be successfully printed in NAG-based photoresists, the writing speed is limited for both photoinitiators. To fabricate a 2D grid at a writing speed of 50 $\mu m\, s^{-1}$ as displayed in Figure 2b, a laser power of already 90% (see Methods) has to be applied when using Irgacure 819. Similar results are obtained, when Irgacure 369 is used. Since higher writing speeds require higher laser power to achieve the same dose, no well-defined 2D structures are obtained at a significantly higher writing speed.

Besides 2D structures also complex 3D architectures can be fabricated with NAG-based resists as shown in Figure 2c revealing a miniaturized 3D model of a rainbow stag beetle [The free 3D model of the beetle is obtained from the website www.ameede.net]. Figure 2d depicts a printed arch consisting of two skewed pillars capped by an architrave. This shows that also free standing 3D structures can be realized underlining the capability of the resist for 3D microprinting.

2.3. Selecting Suitable Sensitizer–Photoinitiator Pairs

As shown in the previous section, the NAG resist can be structured using a single photoinitiator. However, fabricating nonbulky structures requires relatively low writing speeds compared to many other photoresists, which can be printed at several $mm\, s^{-1}$ or even faster.[15]

This disadvantage can be reduced, when a proper sensitizer is added to the photoresist. In general, a sensitizer is also a photoinitiator, but it has to fulfill additional demands (as stated below) to form a sensitizer–photoinitiator pair capable to show a sensitization effect. Therefore, choosing an appropriate sensitizer–photoinitiator pair is conceptionally different from mixing two photoinitiators (as reported elsewhere).[56]

In a sensitizer–photoinitiator pair, the sensitizer and the photoinitiator are distinguished by the following two points. First, at the wavelength used, the sensitizer should possess a higher absorption than the photoinitiator. In the case of DLW-suitable photoresists, the TPCS of the sensitizer should be larger than the TPCS of the photoinitiator. Second, the sensitizer needs a triplet energy, which is higher than that of the photoinitiator. Hence, the energy in the excited triplet state of the sensitizer can be transferred to the triplet state of the photoinitiator initializing the formation of a radical. Meanwhile, the sensitizer returns to the ground state being retained for a new cycle.[42]

Since the photoinitiator is responsible for the initiation of the polymerization, it should be capable to effectively cross-link the monomer. This is the case for Irgacure 369 and Irgacure 819 as shown in the previous section, so these compounds can be considered as the photoinitiator part of the sensitizer–photoinitiator pair.

To find appropriate candidates for the sensitizer part, the triplet energy is taken into account. Irgacure 369 and Irgacure 819 possess a triplet energy of 251 and 232 $kJ\, mol^{-1}$,[41] respectively, thus isopropylthioxanthone (ITX, 257 $kJ\, mol^{-1}$[41]) and benzophenone (BP, 289 $kJ\, mol^{-1}$[41]) are identified as possible sensitizers. However, to act as a sensitizer they also have to provide a higher TPCS than the photoinitiators.

The TPCS of the chosen photoinitiators (Irgacure 369, 819) and sensitizers (ITX, BP) are measured using an open aperture z-scan setup (see Methods). In short, a cuvette containing a solution of the respective substance is moved through the focal spot of a laser beam along the axial direction while the transmittance is collected as a function of the scan position. Hence, the laser intensity dependent absorption is recorded yielding direct access to the TPA coefficient.[57,58] To validate the setup the known TPCS of Rhodamine 6G (Rh6G) in methanol at 780 nm is used as reference.[58] Measuring the TPCS of Rh6G (see **Figure 3**a) reveals a value of 17 GM (Goeppert Mayer) in good accordance with the literature value of 16 GM.

Since the TPCS depends also on the solvent,[58] the photoinitiators and sensitizers of interest are dissolved in DMSO, which is used to mix the photoresists. Measuring at 780 nm (the wavelength applied for DLW) BP does not show any TPA up to the maximum peak intensity of our setup and is therefore not applicable as sensitizer. However, ITX reveals a TPCS of 2 GM, which is indeed remarkably higher than the TPCS for Irgacure 369 and 819, which are both in the range of 0.6–0.7 GM, as it can be discerned in Figure 3b–d. Note that the peak intensity for both Irgacure initiators has to be increased by a factor of two compared to ITX to obtain the characteristic dip. This result is in accordance with the expectations since ITX possesses its TPA maximum at 760 nm while Irgacure 369 and 819 reach their TPA maxima at 670 and 600 nm, respectively.[59] After identification of ITX as a suitable sensitizer, two sensitizer–photoinitiator pairs are tested, consisting of either ITX and Irgacure 369 or ITX and Irgacure 819.

2.4. Sensitization Effect for Two-Photon Polymerization

To investigate the impact of the sensitization effect on two-photon polymerization, various photoresists are mixed (see Methods, Preparation of Photoresists) containing either Irgacure 369, 819 or ITX as well as one of the two sensitizer–photoinitiator pairs mentioned earlier. For a fair comparison between the different resists, the sum of sensitizer and photoinitiator molecules in the resists containing a sensitizer–photoinitiator pair is equal to the amount of photoinitiator molecules in the other resists. In addition, only structures written at

© 2023 The Authors. Advanced Engineering Materials published by Wiley-VCH GmbH

15272648, 2023, 11, Downloaded from https://onlinelibrary.wiley.com/doi/10.1002/adem.202201688 by Rheinland-Pfälzische Technische Universität Kaiserslautern-Landau, Wiley Online Library on [22/04/2024]. See the Terms and Conditions (https://onlinelibrary.wiley.com/terms-and-conditions) on Wiley Online Library for rules of use; OA articles are governed by the applicable Creative Commons License

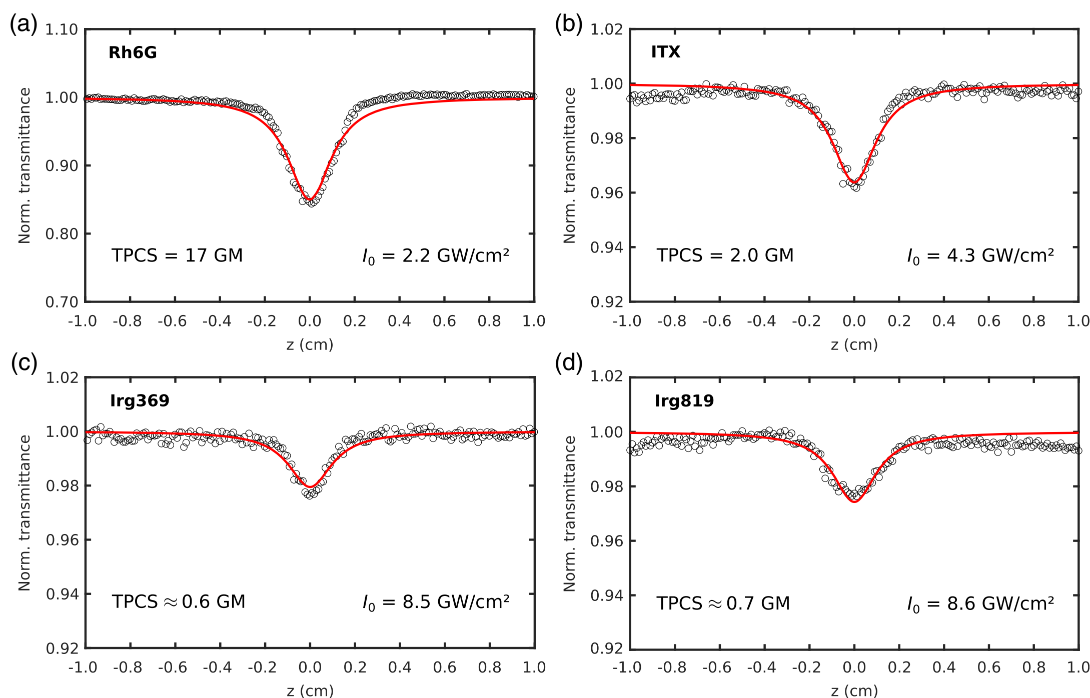

Figure 3. a–d) Open aperture z-scan measurement at 780 nm of (a) Rhodamine 6 G in MeOH, (b) ITX in DMSO, (c) Irgacure 369 in DMSO, and (d) Irgacure 819 in DMSO. As stated in the subfigures, the intensity at the focus I_0 is adjusted to account for different two-photon absorption strengths. Note that the ordinate in (a) is scaled differently from (b)–d) to improve visibility of the characteristic dip in all cases.

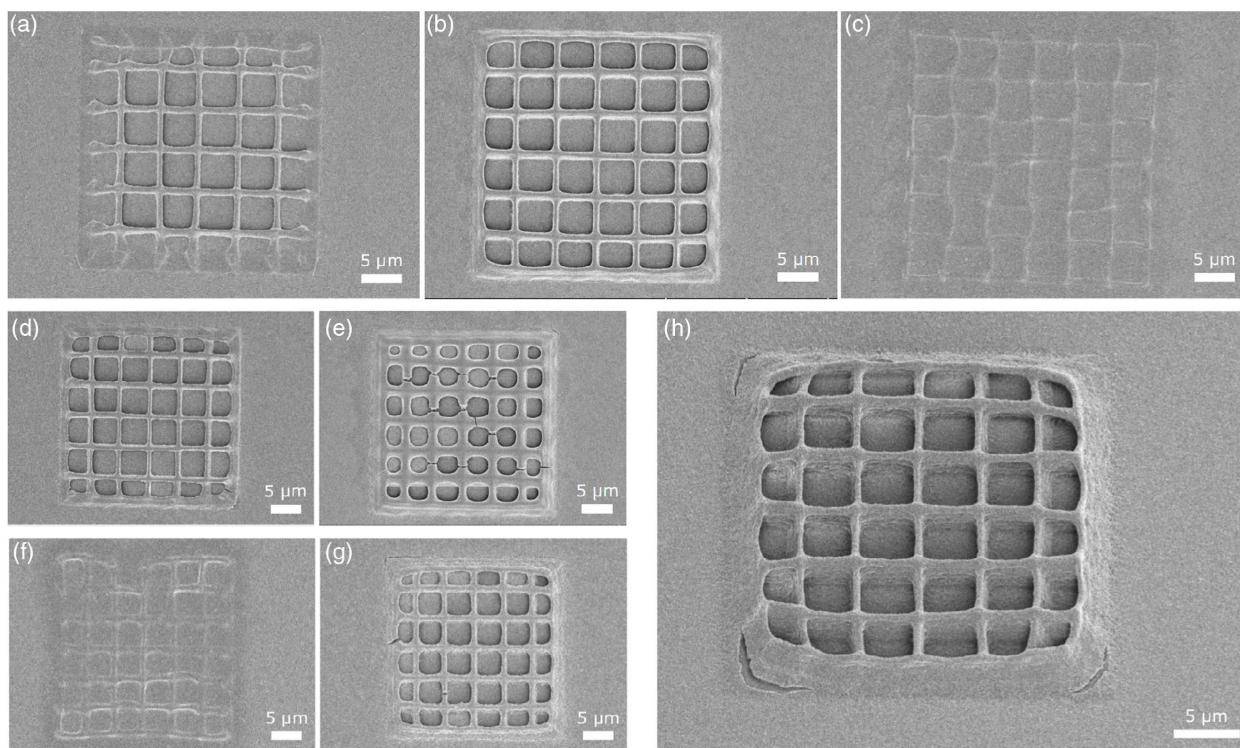

Figure 4. SEM micrographs. a–c) Direct laser written 2D grid structure in a resist containing (a) Irgacure 369, (b) a combination of Irgacure 369 and ITX, and (c) ITX. All grids are written at a speed of 20 μm s^{-1} and 30% laser power. d,e) Fabrication of the same structure using (d) Irgacure 369 and (e) a mixture of Irgacure 369 and ITX at a writing speed of 20 μm s^{-1} and 50% laser power. f,g) Printed grids for a resist containing (f) Irgacure 819 and (g) the combination of Irgacure 819 and ITX. The writing speed is 50 μm s^{-1} and a laser power of 40% is used. h) Grid fabricated in the same resist at 500 μm s^{-1} and 50% laser power. TheSEM image depicts a side view at an angle of 30°.

© 2023 The Authors. Advanced Engineering Materials published by Wiley-VCH GmbH

15272648, 2023, 11, Downloaded from https://onlinelibrary.wiley.com/doi/10.1002/adem.202201688 by Rheinland-Pfälzische Technische Universität Kaiserslautern-Landau, Wiley Online Library on [22/04/2024]. See the Terms and Conditions (https://onlinelibrary.wiley.com/terms-and-conditions) on Wiley Online Library for rules of use; OA articles are governed by the applicable Creative Commons License

the same writing condition, i.e., writing speed and laser power, are directly compared to each other.

Figure 4a–c shows a two-dimensional grid of lines written in a resist containing only Irgacure 369 (a), a mixture of Irgacure 369 and ITX with a ratio of 3:1 (b), and pure ITX (c). For Irgacure 369 and the sensitizer–photoinitiator pair raised lines can be clearly seen at a laser power of 30% and a writing speed of $20\,\mu m\,s^{-1}$. In contrast, almost no lines are observed when the sensitizer is used alone under the same writing conditions. As shown by the weak contrast between the lines and the substrate (see Figure 4c), there is only a tendency of forming lines indicating that higher laser power is needed to form actual solid structures. Indeed, applying laser power close to 100%, it is also possible to achieve solid lines using ITX.

However, comparing Figure 4a,b reveals that the sensitizer–photoinitiator pair clearly outperforms Irgacure 369 in terms of structure quality, as it is recognizable, for example, at the edge of the grid where several lines are missing in Figure 4a. This demonstrates that the combination of a photoinitiator and a sensitizer is highly advantageous over using either solely the photoinitiator or the sensitizer. The advantage arises from the fact that due to the sensitization effect the same dose leads to a higher amount of radicalized Irgacure 369 molecules when a sensitizer is added.

Indeed, increasing the laser power to 50% and thus generating more Irgacure 369 radicals enables a similar structure quality using solely Irgacure 369, as it can be observed in Figure 4d. In contrary, the same laser dose results in a considerably overexposure of the lines in case of the sensitizer–photoinitiator pair, as shown in Figure 4e. This shows that the utilization of the sensitization effect actually lowers the required dose, which is favorable since the available dose at a certain writing speed is limited by the used laser source.

The sensitization effect is not restricted to one certain photoinitiator–sensitizer pair and writing condition. Figure 4f,g shows a grid structure fabricated with only Irgacure 819 and the corresponding sensitizer–photoinitiator pair, respectively. Here, a writing speed of $50\,\mu m\,s^{-1}$ and a laser power of 40% are used. At these conditions, no raised lines are observable using solely Irgacure 819, Figure 4f. However, for a laser power of 90%, it is also possible to write solid structures using Irgacure 819, as shown in Figure 2b. In contrast, the sensitizer–photoinitiator pair enables structure fabrication already at a 40% laser power where neither Irgacure 819 nor ITX alone yield similar results, as shown in Figure 4g.

It should be noted that the ratio between Irgacure 819 and ITX is 7:1 for the presented resist, delivering a further proof that the sensitization effect also works for two-photon polymerization. Since the sensitizer just transfers the absorbed energy without being destroyed in general, it is expected that the sensitization effect occurs already for a small addition of sensitizer.

Due to the required laser dose, the maximum writing speed for nonbulky structures is limited to $\approx 50\,\mu m/s$ using a single photoinitiator. Applying the sensitization effect lowers the required dose and hence greatly enhances the possible writing speed. Figure 4h shows a grid printed at $500\,\mu m\,s^{-1}$ and 50% laser power using the resist containing a mixture of Irgacure 819 and ITX. Thus, the writing speed can be increased by an order of magnitude for the investigated NAG resist underlining the benefit of the sensitization effect for two-photon polymerization and DLW.

3. Conclusions

We have synthesized a novel functionalized derivative of NAG, which enables the fabrication of three-dimensional microarchitectures using DLW. Thus, the range of available animal carbohydrate-based photoresists is expanded to organic solvent-based formulations. Combining hydrogel and nonhydrogel photoresists in a multimaterial printing approach might allow for new functionalities through swelling and shrinking of selective structure parts upon hydration and dehydration. This could enable the fabrication of novel soft robots being entirely based on bio-sourced materials.[60,61] In addition, the successful establishment of a NAG-based photoresist is an important step toward developing new resists utilizing more complex animal-based biopolymers such as chitin. Since chitin is widely spread in the animal kingdom because of its mechanical and optical properties, the possibility to print 3D chitin structures on the micro- and nano-scale might be helpful to analyze functionalities found in nature as well as enable their implementation as biomimetic materials.

While the methacrylated NAG can be cross-linked using a single photoinitiator, it is demonstrated that the addition of a sensitizer substantially improves the quality of the printed structure and enables remarkably higher fabrication speed. This underlines that the sensitization effect known from pigmented UV curing can be successfully transferred from one-photon to TPA processes for the first time and hence become beneficial for DLW. Moreover, the effect is not limited to one specific sensitizer–photoinitiator pair indicating that sensitization is an universal effect also in case of TPA. Therefore, many other sensitizer–photoinitiator pairs might be found possibly outperforming the presented pairs or even enabling the use of photoinitiators, which are currently inaccessible due to a diminishing TPCS at the wavelengths typically applied in commercial DLW systems.

4. Experimental Section

Synthesis of the Photo-Crosslinkable NAG: 3.05 g of NAG (Alfa Aesar, Germany) was dissolved in 100 mL dimethylformamide ($\geq$ 98%, VWR Chemicals, Germany) at 58°C under permanent stirring and reflux conditions. After the solution was allowed to cool to RT, 5.8 mL methacrylic acid anhydride (94%, Sigma-Aldrich, Germany), 0.1 g 4-dimethylaminopyridine (DMAP, 99%, Acros Organics, USA), and 4.04 g *N,N*-dicyclohexylcarbodiimide (DCC, 99%, Alfa Aesar, Germany) were added. The reaction was performed under permanent stirring for 45 h. Subsequently, the reaction mixture was concentrated by employing a rotary evaporator. The methacrylated NAG was then precipitated in an excess of diethyl ether (technical, VWR Chemicals, Germany) within an ice bath. The product was washed five times with diethyl ether and once with ethanol using a centrifuge at 4000 rpm at 20°C for 20 min. Finally, the methacrylated NAG was obtained after evaporating the solvent by employing a rotary evaporator. All chemicals were used as received without further purification.

UV Curing: For the preparation of the photoresist, 50.0 mg MANAG were dissolved in 250 μL dimethyl sulfoxide. Subsequently, 1 mg Irgacure 369 was added under stirring for 30 min. Then, the photoresist was irradiated simultaneously with wavelengths of 254 nm and 365 nm for

© 2023 The Authors. Advanced Engineering Materials published by Wiley-VCH GmbH

15272648, 2023, 11, Downloaded from https://onlinelibrary.wiley.com/doi/10.1002/adem.202201688 by Rheinland-Pfälzische Technische Universität Kaiserslautern-Landau, Wiley Online Library on [22/04/2024]. See the Terms and Conditions (https://onlinelibrary.wiley.com/terms-and-conditions) on Wiley Online Library for rules of use; OA articles are governed by the applicable Creative Commons License

30 min, whereas the sample was placed 5 cm away from the UV light source. UV-induced crosslinking was performed with a 8 W UV lamp (Herolab, Germany).

Fourier Transform Infrared Spectroscopy: Fourier transform infrared spectra were recorded on the powder of NAG and functionalized NAG using a Frontier MIR spectrometer (L1280018) performed with an attenuated total reflection (ATR) diamond (PerkinElmer, Germany). The spectra were recorded between 4000 and 400cm^{-1} with a resolution of 4cm^{-1} and at least 8 scans.

NMR Spectroscopy: NMR spectra were acquired on a Jeol ECS-400 NMR (Japan). The evaluation was performed by Delta v 5.0.4 software (Jeol) and MestReNova v 14.2.3 (Mestrelab Research, Spain). Samples were analyzed in dimethyl sulfoxide-d_6 solutions at 25°C.^{13}C NMR spectra were recorded with 2048 scans, whereas ^{1}H NMR spectra were measured with 32 scans.

Elemental Analysis: The elemental composition of the unmodified and modified NAG was measured by a EuroEA-Elemental Analyser (Eurovector, Italy). 1–3 mg powder in tin crucibles was analyzed. This enabled the determination of the degree of methacrylation of NAG.

Z-scan Measurements: For open-aperture *z*-scan measurements, the beam of a femtosecond Ti:Sa laser (Chameleon, Coherent Inc., USA) was focused with a 20 cm focal lens onto a point within the travel range of a motorized stage (Soloist, Aerotech GmbH, Germany). About 10 cm behind the focus, the light was collected with a second lens focusing the light on a detector (DET36A2, Thorlabs Inc., USA). The output of the detector was fed into a lock-in amplifier (SR830 DSP, Standford Research Systems, USA). Thereby, the lock-in amplifier was triggered by an optical chopper (MC2000, Thorlabs Inc.) equipped with a chopper blade with 50% duty cycle, which was placed in the beam path right in front of the first lens. The output signal of the lock-in amplifier as well as the current stage position were sent to a computer and recorded by a self-written LabVIEW program (National Instruments, USA). To measure the TPCS of the photoinitiators, they are dissolved in DMSO (Sigma-Aldrich) in a concentration of 0.05 M, filled into a cuvette with 1 mm optical path length (Hellma GmbH & Co. KG, Germany) and scanned through the focus of the laser beam using the stage. In addition, Rhodamine 6G (Acros Organics) dissolved in the same concentration in methanol (VWR International GmbH, Germany) was used as a reference. The TPA coefficient β can be obtained from the measured normalized transmittance curve by fitting with the equation $T = 1 - \frac{\beta I_0 L}{2^{3/2}(1+(z^2/z_0^2))}$, where I_0 is the peak intensity at the focus, L is the sample thickness, and z_0 is the diffraction length. Except for β,all other quantities depended only on the setup and were accessible as explained in more detail elsewhere.[57,58] The TPCS was directly related to β via $\text{TPCS} = \frac{\beta h\nu \times 10^3}{N_A c}$ with frequency ν of the used laser, the Avogadro constant N_A and the concentration of photoinitiator c.[58] All results were given in the common unit Goeppert Mayer (GM).

Preparation of Photoresists: Prior to mixing, the photoresists different stock solutions were prepared. The stock solutions contained DMSO (Sigma-Aldrich) and either Irgacure 369, Irgacure 819 (both TCI chemicals, Japan) or ITX (Sigma-Aldrich) each in a concentration of 0.05 M. All stock solutions were stirred until the photoinitiator was completely dissolved. For mixing the photoresists, first, the required amount of functionalized NAG was weighed. Subsequently, stock solution was added until a concentration of 250 g NAG per liter stock solution was reached. For resists containing only one photoinitiator, the stock solutions were added as prepared. For the both sensitizer–photoinitiator pairs, the stock solutions were first mixed in a ratio of 3:1 (Irgacure 369 to ITX solution) as well as 7:1 (Irgacure 819 to ITX solution) before adding the mixture to the NAG. Afterward, the resists were stirred overnight using a magnetic stirrer. To avoid the inclusion of unsolved particles, the resists were finally transferred to a reaction vial and separated for 20 min in a centrifuge (Mini-Zentrifuge, Carl Roth GmbH + Co. KG, Germany).

Direct Laser Writing: All structures were printed with a Photonic Professional GT (Nanoscribe GmbH, Germany) operating at a wavelength of 780 nm with a laser power of 57.8 mW (=100%). The photoresists were extracted from the vial using a syringe and a drop of resist was placed on top of a 170 μm-thick glass substrate (Gerhard Menzel GmbH, Germany). The top side of the substrate was coated with a thin layer of aluminum oxide using atomic layer deposition (R-200 Standard, Picosun Oy., Finland) to enable easier detection of the glass-resist interface. The used sample holder allowed for placing an uncoated coverslip slightly above the substrate sandwiching the resist in between. This was done because DMSO is hygroscopic with the detrimental effect of blurring the resist if it was exposed to air too long. During writing, the laser beam was focused into the resist through the substrate, using a drop of immersion oil (Immersol 518F, Carl Zeiss AG, Germany) between the objective (63×, NA = 1.4) and the bottom of the substrate. After printing, the samples were developed for 90 min in DMSO and subsequently for 10 min in acetone. For 2D grids and lines, the samples were carefully blown dry with a nitrogen pistol. The printed 3D structures were dried using a critical point dryer (EM CPD300, Leica Microsystems GmbH, Germany).

Supporting Information

Supporting Information is available from the Wiley Online Library or from the author.

Acknowledgements

D.T.M. and M.R. contributed equally to this work. The authors gratefully acknowledge financial support from the German Research Foundation DFG within the priority program "Tailored Disorder—A science- and engineering-based approach to materials design for advanced photonic applications" (SPP 1839). The authors thank the team of the Nano Structuring Center (NSC) at the RPTU Kaiserslautern-Landau for their support with scanning electron microscopy. [Correction added on 13 February 2023, after first online publication: Georg von Freyman was assigned as corresponding author.]

Open Access funding enabled and organized by Projekt DEAL.

Conflict of Interest

The authors declare no conflict of interest.

Data Availability Statement

The data that support the findings of this study are available from the corresponding author upon reasonable request.

Keywords

bio-based photoresist, direct laser writing, methacrylated N-acetyl-D-glucosamine, monosaccharide, sensitization effect

Received: December 16, 2022
Published online: January 31, 2023

[1] S. Maruo, O. Nakamura, S. Kawata, *Opt. Lett.* **1997**, *22*, 132.
[2] T. Gissibl, S. Thiele, A. Herkommer, H. Giessen, *Nat. Commun.* **2016**, *7*, 11763.
[3] A. Kubec, M.-C. Zdora, U. T. Sanli, A. Diaz, J. Vila-Comamala, C. David, *Nat. commun.* **2022**, *13*, 1305.
[4] J. Li, S. Thiele, R. W. Kirk, B. C. Quirk, A. Hoogendoorn, Y. C. Chen, K. Peter, S. J. Nicholls, J. W. Verjans, P. J. Psaltis, C. Bursill, A. M. Herkommer, H. Giessen, R. A. McLaughlin, *Small* **2022**, *18*, 2107032.

 © 2023 The Authors. Advanced Engineering Materials published by Wiley-VCH GmbH

15272648, 2023, 11, Downloaded from https://onlinelibrary.wiley.com/doi/10.1002/adem.202201688 by Rheinland-Pfälzische Technische Universität Kaiserslautern-Landau, Wiley Online Library on [22/04/2024]. See the Terms and Conditions (https://onlinelibrary.wiley.com/terms-and-conditions) on Wiley Online Library for rules of use; OA articles are governed by the applicable Creative Commons License

[5] A. K. Au, W. Huynh, L. F. Horowitz, A. Folch, *Ange. Chem., Int. Ed.* **2016**, *55*, 3862.
[6] A. Lüken, M. Geiger, L. Steinbeck, A.-C. Joel, A. Lampert, J. Linkhorst, M. Wessling, *Adv. Healthcare Mater.* **2021**, *10*, 2100898.
[7] C. Michas, M. Ç. Karakan, P. Nautiyal, J. G. Seidman, C. E. Seidman, A. Agarwal, K. Ekinci, J. Eyckmans, A. E. White, C. S. Chen, *Sci. Adv.* **2022**, *8*, 16.
[8] M. Rothammer, C. Zollfrank, K. Busch, G. von Freymann, *Adv. Opt. Mater.* **2021**, *9*, 2100787.
[9] Y. Wang, Z. Li, M. Elhebeary, R. Hensel, E. Arzt, M. T. A. Saif, *Sci. Adv.* **2022**, *8*, 12.
[10] R. C. R. Pompe, D. T. Meiers, W. Pfeiffer, G. von Freymann, *Adv. Opt. Mater.* **2022**, *10*, 2200700.
[11] J. K. Hohmann, G. von Freymann, *Adv. Funct. Mater.* **2014**, *24*, 6573.
[12] J. Jang, J.-y. Kim, Y. C. Kim, S. Kim, N. Chou, S. Lee, Y.-H. Choung, S. Kim, J. Brugger, H. Choi, J. H. Jang, *Adv. Healthcare Mater.* **2019**, *8*, 1900379.
[13] Q. Akolawala, M. Rovituso, H. H. Versteeg, A. M. Rondon, A. Accardo, *ACS Appl. Mater. Interfaces* **2022**, *14*, 20778.
[14] J. K. Hohmann, M. Renner, E. H. Waller, G. von Freymann, *Adv. Opt. Mater.* **2015**, *3*, 1488.
[15] P. Kiefer, V. Hahn, M. Nardi, L. Yang, E. Blasco, C. Barner-Kowollik, M. Wegener, *Adv. Opt. Mater.* **2020**, *8*, 2000895.
[16] M. Schmid, D. Ludescher, H. Giessen, *Opt. Mater. Express* **2019**, *9*, 4564.
[17] J. Durisova, D. Pudis, M. Goraus, P. Gaso, *Appl. Surf. Sci.* **2018**, *461*, 108.
[18] L. Pertoldi, V. Zega, C. Comi, R. Osellame, *J. Appl. Phys.* **2020**, *128*, 175102.
[19] F. Mayer, D. Ryklin, I. Wacker, R. Curticean, M. Čalkovský, A. Niemeyer, Z. Dong, P. A. Levkin, D. Gerthsen, R. R. Schröder, M. Wegener, *Adv. Mater.* **2020**, *32*, 2002044.
[20] J. Bauer, C. Crook, A. G. Izard, Z. C. Eckel, N. Ruvalcaba, T. A. Schaedler, L. Valdevit, *Matter* **2019**, *1*, 1547.
[21] E. S. Farrell, N. Ganonyan, I. Cooperstein, M. Y. Moshkovitz, Y. Amouyal, D. Avnir, S. Magdassi, *Appl. Mater. Today* **2021**, *24*, 101083.
[22] T. Tanaka, A. Ishikawa, S. Kawata, *Appl. Phys. Lett.* **2006**, *88*, 081107.
[23] E. H. Waller, G. von Freymann, *Nanophotonics* **2018**, *7*, 1259.
[24] A. Nishiguchi, A. Mourran, H. Zhang, M. Möller, *Adv. Sci.* **2018**, *5*, 1700038.
[25] M. Hippler, E. Blasco, J. Qu, M. Tanaka, C. Barner-Kowollik, M. Wegener, M. Bastmeyer, *Nat. Commun.* **2019**, *10*, 232.
[26] F. Kotz, A. S. Quick, P. Risch, T. Martin, T. Hoose, M. Thiel, D. Helmer, B. E. Rapp, *Adv. Mater.* **2021**, *33*, 2006341.
[27] M. Rothammer, M.-C. Heep, G. von Freymann, C. Zollfrank, *Cellulose* **2018**, *25*, 6031.
[28] E. Skliutas, M. Lebedevaite, S. Kasetaite, S. Rekštytė, S. Lileikis, J. Ostrauskaite, M. Malinauskas, *Sci. Rep.* **2020**, *10*, 9758.
[29] S. Grauzeliene, A. Navaruckiene, E. Skliutas, M. Malinauskas, A. Serra, J. Ostrauskaite, *Polymers* **2021**, *13*, 872.
[30] D. Serien, K. Sugioka, *Opto-Electron. Adv.* **2018**, *1*, 180008.
[31] O. Kufelt, A. El-Tamer, C. Sehring, S. Schlie-Wolter, B. N. Chichkov, *Biomacromolecules* **2014**, *15*, 650.
[32] O. Kufelt, A. El-Tamer, C. Sehring, M. Meißner, S. Schlie-Wolter, B. N. Chichkov, *Acta Biomater.* **2015**, 186.
[33] A. Berg, R. Wyrwa, J. Weisser, T. Weiss, R. Schade, G. Hildebrand, K. Liefeith, B. Schneider, R. Ellinger, M. Schnabelrauch, *Adv. Eng. Mater.* **2011**, *13*, B274.
[34] C. Loebel, N. Broguiere, M. Alini, M. Zenobi-Wong, D. Eglin, *Biomacromolecules* **2015**, *16*, 2624.
[35] J. Torgersen, X.-H. Qin, Z. Li, A. Ovsianikov, R. Liska, J. Stampfl, *Adv. Funct. Mater.* **2013**, *23*, 4542.
[36] S. You, J. Li, W. Zhu, C. Yu, D. Mei, S. Chen, *J. Mater. Chem. B* **2018**, *6*, 2187.
[37] M. G. Rao, P. Bharathi, R. Akila, *Sci. Revs. Chem. Commun* **2014**, *4*, 61.
[38] T. B. Schroeder, J. Houghtaling, B. D. Wilts, M. Mayer, *Adv. Mater.* **2018**, *30*, 1705322.
[39] M. Rothammer, D. T. Meiers, M. Maier, G. von Freymann, C. Zollfrank (Preprint) arXiv:2211.01271, v1, submitted: Nov. **2022**.
[40] L. Brigo, A. Urciuolo, S. Giulitti, G. Della Giustina, M. Tromayer, R. Liska, N. Elvassore, G. Brusatin, *Acta Biomater.* **2017**, *55*, 373.
[41] W. A. Green, *Industrial Photoinitiators: A Technical Guide*, CRC Press, Boca Raton, FL **2010**.
[42] G. Rist, A. Borer, K. Dietliker, V. Desobry, J. Fouassier, D. Ruhlmann, *Macromol.* **1992**, *25*, 4182.
[43] C. She, N. Dinh, A. T. Tu, *Biochim. Biophys. Acta, Gen. Subj.* **1974**, *372*, 345.
[44] S. Belfer, Y. Purinson, O. Kedem, *Acta Polym.* **1998**, *49*, 574.
[45] J. A. Alkrad, Y. Mrestani, D. Stroehl, S. Wartewig, R. Neubert, *J. Pharm. Biomed. Anal.* **2003**, *31*, 545.
[46] Q. Wang, L. Ren, C. Xu, Z. Zhai, J.-a. Zhou, Y. Yao, H. Xia, Y. Wang, *J. Appl. Polym. Sci.* **2013**, *128*, 89.
[47] X. Chen, Y. Liu, F. M. Kerton, N. Yan, *RSC Adv.* **2015**, *5*, 20073.
[48] Y. Ji, X. Yang, Z. Ji, L. Zhu, N. Ma, D. Chen, X. Jia, J. Tang, Y. Cao, *ACS Omega* **2020**, *5*, 8572.
[49] S. Bonnin, F. Besson, M. Gelhausen, S. Chierici, B. Roux, *FEBS Lett.* **1999**, *456*, 361.
[50] K. H. Sizeland, K. A. Hofman, I. C. Hallett, D. E. Martin, J. Potgieter, N. M. Kirby, A. Hawley, S. T. Mudie, T. M. Ryan, R. G. Haverkamp, M. H. Cumming, *Materialia* **2018**, *3*, 90.
[51] Y. Du, H. Zang, Y. Feng, K. Wang, Y. Lv, Z. Liu, *J. Mol. Liq.* **2022**, *347*, 117970.
[52] T. Cebe, N. Ahuja, F. Monte, K. Awad, K. Vyavhare, P. Aswath, J. Huang, M. Brotto, V. Varanasi, *J. Mater. Res.* **2020**, *35*, 58.
[53] E. Khor, H. Wu, L. Y. Lim, C. M. Guo, *Materials* **2011**, *4*, 1728.
[54] C.-H. Dang, C.-H. Nguyen, T.-D. Nguyen, C. Im, *RSC Adv.* **2014**, *4*, 6239.
[55] C. Ramilo, R. J. Appleyard, C. Wanke, F. Krekel, N. Amrhein, J. N. Evans, *Biochemistry* **1994**, *33*, 15071.
[56] D. Serien, S. Takeuchi, *J. Laser Micro/Nanoeng.* **2017**, *12*, 80.
[57] M. Sheik-Bahae, A. A. Said, T.-H. Wei, D. J. Hagan, E. W. Van Stryland, *IEEE J. Quantum Electron.* **1990**, *26*, 760.
[58] A. Nag, D. Goswami, *J. Photochem. Photobiol., A* **2009**, *206*, 188.
[59] K. J. Schafer, J. M. Hales, M. Balu, K. D. Belfield, E. W. Van Stryland, D. J. Hagan, *J. Photochem. Photobiol., A* **2004**, *162*, 497.
[60] Y. Lee, W. Song, J.-Y. Sun, *Mater. Today Phys.* **2020**, *15*, 100258.
[61] G. Stano, G. Percoco, *Extreme Mech. Lett.* **2021**, *42*, 101079.

 © 2023 The Authors. Advanced Engineering Materials published by Wiley-VCH GmbH

15272648, 2023, 11, Downloaded from https://onlinelibrary.wiley.com/doi/10.1002/adem.202201688 by Rheinland-Pfälzische Technische Universität Kaiserslautern-Landau, Wiley Online Library on [22/04/2024]. See the Terms and Conditions (https://onlinelibrary.wiley.com/terms-and-conditions) on Wiley Online Library for rules of use; OA articles are governed by the applicable Creative Commons License